



Original article

Further insights into the SAR of α -substituted cyclopropylamine derivatives as inhibitors of histone demethylase KDM1A

Marco Pieroni ^{a,1}, Giannamaria Annunziato ^{a,1}, Elisa Azzali ^a, Paola Dessanti ^b,
Ciro Mercurio ^b, Giuseppe Meroni ^b, Paolo Trifiró ^b, Paola Vianello ^b, Manuela Villa ^b,
Claudia Beato ^a, Mario Varasi ^b, Gabriele Costantino ^{a,*}

^a Dipartimento Farmaceutico, University of Parma, Parco Area delle Scienze 27/A, Parma 43124, Italy

^b Drug Discovery Unit, European Institute of Oncology, Via Adamello 16, 20139 Milan, Italy

ARTICLE INFO

Article history:

Received 8 October 2014

Received in revised form

21 November 2014

Accepted 19 December 2014

Available online 7 January 2015

Keywords:

Lysine demethylase

Tranylcypromine

Epigenetic

ABSTRACT

Epigenetics alterations including histone methylation and acetylation, and DNA methylation, are thought to play important roles in the onset and progression of cancer in numerous tumour cell lines. Lysine-specific demethylase 1 (LSD1 or KDM1A) is highly expressed in different cancer types and inhibiting KDM1A activity seems to have high therapeutic potential in cancer treatment.

In the recent years, several inhibitors of KDM1A have been prepared and disclosed. The majority of these derivatives were designed based on the structure of tranylcypromine, as the cyclopropane core is responsible for the covalent interaction between the inhibitor and the catalytic domain of KDM proteins. In this study, we have further extended the SAR regarding compounds **1a–e**, which were recently found to inhibit KDM1A with good activity. The decoration of the phenyl ring at the β -position of the cyclopropane ring with small functional groups, mostly halogenated, and in particular at the *meta* position, led to a significant improvement of the inhibitory activity against KDM1A, as exemplified by compound **44a**, which has a potency in the low nanomolar range (31 nM).

© 2015 Elsevier Masson SAS. All rights reserved.

1. Introduction

The control of gene expression, as well as the normal development and maintenance of tissue specific patterns, are regulated by epigenetic modifications [1,2]. Several chemical reactions such as acetylation, methylation, phosphorylation, ubiquitination or sumoylation, modify the architecture of histone proteins, leading to activation/deactivation of portions of chromatin [3,4].

As such, pharmacological control of epigenetic modifications might represent a valuable means to prevent the onset and the progression of many lethal pathologies [5]. Indeed, the release to the market of Zolanza (vorinostat) [6], and Istodax (romidepsin) [7], two pan-HDAC inhibitors indicated for the treatment of cutaneous

T-cell lymphoma, accounts for the trustworthiness of the epigenetic approach in the treatment of specific types of cancer.

Along with histone deacetylases (HDAC), the widest studied class of epigenetic controllers [8,9], and a number of bromodomain-containing proteins [10], histone lysine demethylases (KDMs) are gaining increasing consideration as valuable therapeutic targets [11]. Methylation of histones, in particular H3 and H4, is an important way to access to the tightly condensed chromatin, therefore influencing gene expression and genomic stability. The process of histone lysine methylation is not steady, but it is rather regulated by the dynamic addition and removal of up to three methyl units on the lysine amino moiety. Depending on the site and the degree of histone methylation (mono-, di-, trimethylation), KDMs can either activate or repress transcription of genes, allowing for a fine-tuning of several physiological and pathological processes [12,13]. So far, two classes of KDMs have been discovered, based on their mechanism of action: a) flavin-dependent histone KDMs, having mono- and di-methylated lysines as the substrate; and b) jumonji domain-containing protein (JMJD) histone KDMs, which are Fe(II) and α -oxoglutarate dependent oxygenases and are effective also toward tri-methylated

Abbreviations: BOC, *t*-butyloxycarbonyl; DIPEA, *N,N*-diisopropylethylamine; DMF, *N,N*-dimethyl formamide; DMSO, dimethylsulfoxide; HDAC, histone deacetylase; KDM1A, lysine-specific histone demethylase type 1; MAO, monoamine oxidase; PCPA, phenylcyclopropylamine; TEA, triethylamine.

* Corresponding author.

E-mail address: gabriele.costantino@unipr.it (G. Costantino).

¹ These authors contributed equally to this work.

lysines [14–17]. The former class can be further divided into two additional sub-families: lysine specific demethylase 1 (LSD1 or KDM1A) and lysine specific demethylase 2 (LSD2 or KDM1B) [18,19]. KDM1A, the first histone demethylase discovered, selectively demethylates the mono- or di-methylated lysine 4 of histone H3 (H3K4), along with other lysines present in proteins of therapeutic interest such as p53, DNA methyltransferase 1, STAT3, E2F1 and MYPT1 [19]. Overexpression of KDM1A has been observed in numerous types of cancer, including acute myeloid leukaemia [20], neuroblastoma [21], as well as prostate, bladder, lung, liver and colorectal cancer [22]. In light of these evidences, inhibition of KDM1A can be considered an effective strategy to thwart crucial proliferative pathways in many types of tumour.

Since the discovery of KDM1A, several inhibitors have been reported [23]. Because of the similarities between the KDM1A catalytic domain and that of other amino-oxidases, it is not surprising that tranlycypromine (*trans*-2-phenylcyclopropylamine, **PCPA**), a monoamine oxidase (MAO) inhibitor that binds covalently to the cofactor FAD, is also a KDM1A inhibitor ($IC_{50} = 11.6 \mu M$) [24]. Therefore, the majority of KDM1A inhibitors known so far embody a tranlycypromine-like scaffold variously substituted, in order to improve the overall potency and the selectivity toward MAO A and MAO B inhibition. In many cases, (Fig. 1, **A–C**), a remarkable combination of high activity and selectivity was achieved [25–28]. Also other monoamine oxidase (MAO) inhibitors, such as **pargyline**, have been investigated but the issue of the poor pharmacokinetic properties seemed to be unsolvable [29]. Some polyamines (**CGC-11047**) were evaluated as KDM1A inhibitors, with compounds showing activity in the low micromolar range [30,31]. Other compounds, not belonging to any definite series (**namoline**, **CBB-1007**), were found to be reversible KDM1A inhibitors as well [32]. Recently, a series of *N'*-(1-phenylethylidene)-benzohydrazides (**D**), discovered by the virtual screening of a chemical library of 2 million compounds, were found to be selective and reversible inhibitors of KDM1A [33].

To refine this overview, it is worthwhile to report a series of patent applications filed by Oryzon and GSK, disclosing a series of *N*-substituted tranlycypromine derivatives highly active and selective for KDM1A over MAO A and MAO B [34–36]. Two compounds from these series were reported to have entered clinical

studies (<http://www.clinicaltrials.gov/ct2/show/NCT02034123?term=lsd1&rank=3>; www.clinicaltrialsregister.eu/ctr-search/trial/2013-002447-29/ES).

2. Results and discussion

2.1. Rationale

The cyclopropane core of PCPA is essential for inhibition, and it covalently interacts with the FAD cofactor, leading to irreversible enzyme inactivation [17,27,37]. Some of us have recently reported [24] a series of PCPA derivatives carrying a substituent in position α of the cyclopropane, which led to a higher KDM1A inhibitory activity compared to tranlycypromine. Since the encouraging results, we designed a further expansion of α -substituted PCPA derivatives, investigating the effect of small substituents at the β -phenyl group.

The mechanism of action of tranlycypromine involves the formation of a benzyl radical, therefore we reasoned that small electron-withdrawing groups (EWGs) or electron-donating groups (EDGs) could affect the SAR already established toward KDM1A inhibition, and modulate the activity of the derivatives. Some of the synthesized compounds are endowed with a spiroamido moiety aiming at finding out whether the amino group and the substituent in the α -position would share the same enzymatic pocket. The majority of the derivatives synthesized was found to be more active than the corresponding unadorned compounds, providing clear hints about the role of the substituents attached at the β -phenyl ring.

2.2. Chemistry

The title compounds were synthesized through a straightforward protocol already reported [24,38], with the exception of compound **48b** that was synthesized in an alternative route, as reported below. When not commercially available, phosphonates **a–e** were obtained by reacting triethyl phosphonoacetate with the proper bromide, in the presence of NaH as the base, from 0 °C to rt. Phosphonates **a–e** were then deprotonated with butyllithium and reacted with variously substituted styrene oxides (**2**→**15**) in dimethoxyethane at 130 °C, allowing the desired *trans*

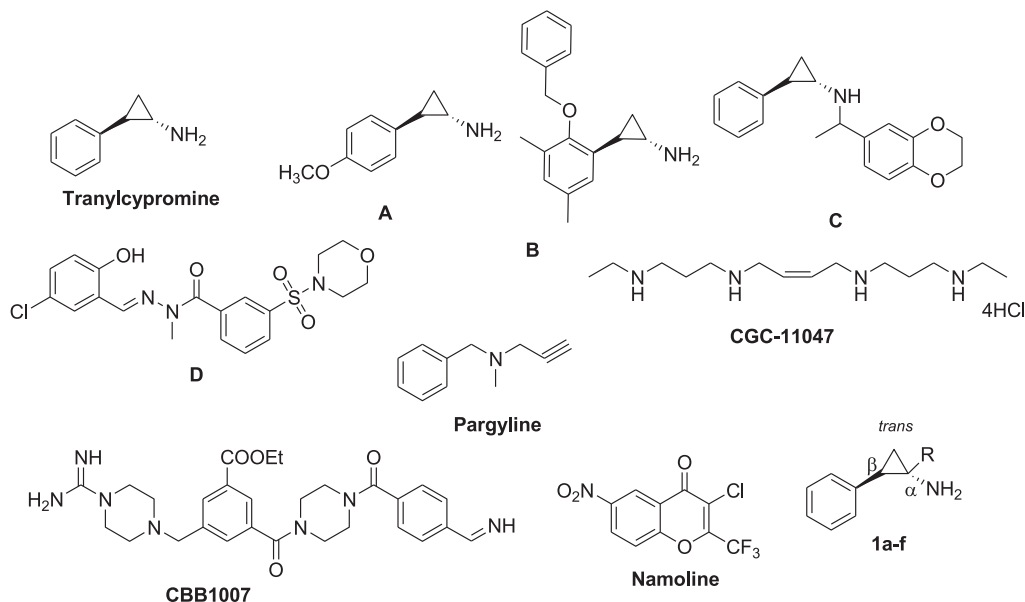


Fig. 1. Tranlycypromine and other known KDM1A inhibitors.

cyclopropanecarboxylic ethyl esters to be obtained. Subsequent basic hydrolysis with LiOH under MW irradiation, followed by Curtius rearrangement with diphenyl phosphorazidate in presence of triethylamine in anhydrous *tert*-butanol at 90 °C, provided the N-BOC protected precursors. Finally, hydrolysis of the carbamates either with 4 N HCl or gaseous HCl in ethyl acetate at room temperature gave the desired amines as hydrochloride salts in variable yields (Scheme 1).

The synthesis of the spiro amides **63** and **66** was achieved through the key intermediate **61**, already reported [39]. Briefly, the inexpensive precursors benzaldehyde and diethyl malonate were first reacted in toluene at 80 °C for 48 h. The use of MW irradiation drastically reduced the reaction time, although with no improvement in the yield. Corey–Chaykovsky cyclopropanation of intermediate **58** with (CH₃)₃SOI in DMSO at room temperature, using NaH as the base, led to compound **59** in good yields. Subsequent selective mono-hydrolysis of the ester moiety with alcoholic NaOH, followed by the Curtius rearrangement, allowed intermediate **61** to be obtained in good overall yields. In this case, the conditions used for the Curtius rearrangement are slightly different from those previously reported, as cyclohexane, and not *tert*-butanol, was used as the solvent. Removal of the BOC protecting group with trifluoroacetic acid yielded the free amine, that is immediately used in the next reaction step without purification nor storage, since the lack of stability of the cyclopropylamino moiety. Reductive amination of unmasked **61** using N-Boc-2-aminoacetaldehyde as the coupling agent, and sodium triacetoxyborohydride as the reducing agent, in dichloroethane and triethylamine, led to compound **62** in modest yields. Hydrolysis of the protective group with trifluoroacetic acid, followed by treatment with NaOH 5 M at room temperature, yielded lactam **63** as a yellowish solid. All of the attempts to reduce the lactam, such as the use of LAH, NaCNBH₄, NaBH₄, and BH₃·THF, failed to provide the spiro-piperidine analogues. The reduction of ester **61**, with excess LAH in dry THF at room temperature, gave the alcohol **64**. BOC deprotection of **64** with trifluoroacetic acid, followed by coupling with 2-bromoacetyl chloride in dichloromethane at 0 °C, gave the amide **65** in moderate yields. The final cyclization of intermediate **65** to give lactam **66** was achieved in good yields using NaH in dichloromethane from 0 °C to room temperature. Also in this case, the numerous attempts to produce the reduced adduct bearing a spiro-morpholine moiety had no success. It can be speculated that, both for compounds **63** and **66**, the peculiar structural constraint given by the spiro-cyclopropane moiety might have played a role in the unsuccessful

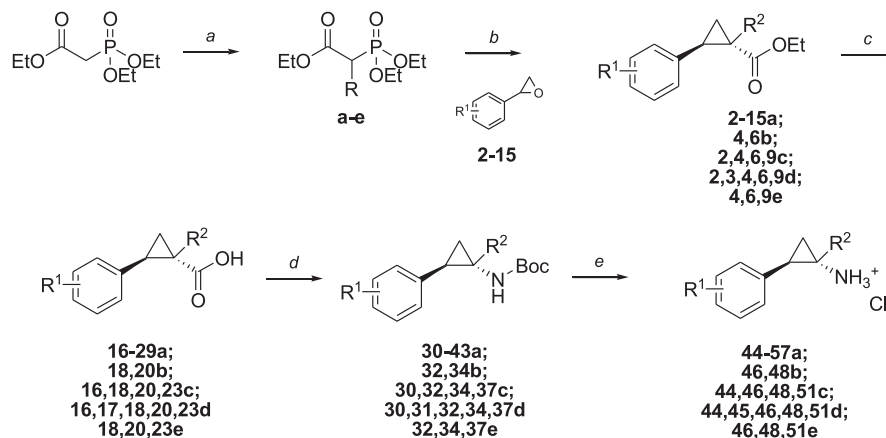
reduction of the lactam, a procedure that is otherwise well documented in the literature for other substrates.

Compound **48b** was prepared starting from the condensation between *p*-chlorobenzaldehyde and 2-phenylacetic acid, to obtain the corresponding 2,3-diphenylacrylic acid **67**, that is esterified with iodomethane in DMSO and KOH. Thus, using the same synthetic route seen in Scheme 2, that is cyclopropanation reaction with trimethylsulfonium iodide, followed by methyl ester hydrolysis, Curtius rearrangement and BOC deprotection, the title compound **48b** is obtained in good yield (Scheme 3).

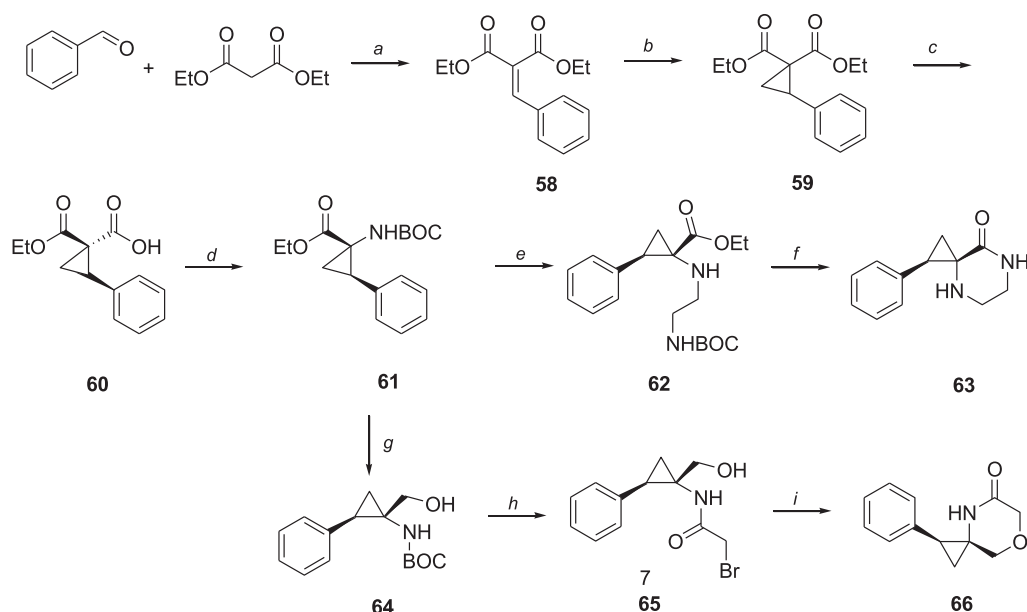
2.3. SAR description

In this study, a total of 29 compounds were prepared and evaluated. KDM1A inhibitory activity was assessed using human recombinant KDM1A/CoREST protein as enzymatic source and a synthetic mono-methylated H3–K4 peptide containing 21 amino acids as the substrate [24]. The compounds were incubated with the enzymatic complex and the results are expressed as IC₅₀. The unadorned derivatives **1a–f** were used as reference compounds (Table 1).

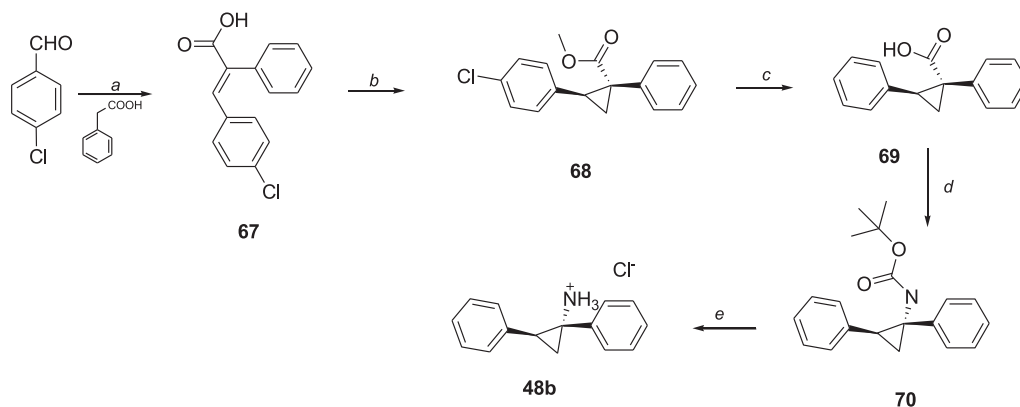
In the previous work we have reported that bulky substituents at the α -position of the cyclopropane core, such as the phenyl (**1b**, IC₅₀ = 0.161 μ M), phenylethyl (**1c**, IC₅₀ = 0.202 μ M) and naphthyl (**1d**, IC₅₀ = 0.218 μ M) resulted to confer better activity compared to small alkyl groups such as ethyl (**1a**, IC₅₀ = 0.779 μ M) and methyl (**1f**, IC₅₀ = 1.72 μ M). For this reason, a preliminary round of modifications at the β -phenyl ring of PCPA was carried out based on the α -phenyl, α -phenylethyl and α -naphthyl scaffolds. Since the mechanism of action involves the formation of a benzyl radical, functional groups with electron withdrawing nature such as halogens were first investigated. When bromine and chlorine were positioned at the *para* position of **1b**, the results were somehow conflicting: while the bromine led to a 4-fold improvement of the activity (**46b** vs **1b**), chlorine led to a decrease of the activity by a similar range (**48b** vs **1b**). Thus, the α -phenylethylcyclopropane scaffold was investigated. Substitution at the *para* position with chlorine or bromine led to a slight improvement of the activity compared to the reference compound (**46c** and **48c** vs **1c**), whereas fluorine did not lead to any significant improvement (**51c**). When similar substitutions were carried out on scaffold **1d**, neither the *para*-bromo substitution nor the *para*-fluoro allowed more potent derivatives to be obtained (**46d**, and **51d** vs **1d**). In particular, the *para*-fluoro was found to be rather detrimental, leading to a 3-fold



Scheme 1. Reagents and conditions: a) NaH, DME, R–Br, reflux, overnight; b) nBuLi, DME, –78 °C to rt, 18 h; c) LiOH, THF/H₂O/MeOH (3:1:1), MW, 100 °C, 10 min; d) diphenylphosphorylazide, triethylamine, *t*BuOH, rt, then reflux; e) HCl (g), dioxane or Ethyl acetate; For R and R' see Table 1; after reaction b compounds are obtained as a mixture of the 2 enantiomers.



Scheme 2. Reagents and conditions: a) piperidine, acetic acid, toluene, reflux, 48 h; b) $(\text{CH}_3)_3\text{SOI}$, NaH, DMSO, rt; c) NaOH, 1 equiv, EtOH, rt 12 h; d) DPPA, TEA, *t*BuOH, hexanes, rt, 16 h; e) 1. TFA/DCM, 1 h; 2. *N*-BOC-acetaldehyde, TEA, NaBH(OAc)₃, DCE, 3 h, another 0.5 equiv of aldehyde is added after 1 h; f) 1. TFA/DCM 1 h; 2. NaOH 5 M/DCM, rt; g) LAH, THF, rt; h) 1. TFA/DCM, 1 h; 2. bromoacetyl chloride, TEA, DCM, 0 °C, 2 h; i) NaH, THF, rt, 4 h.



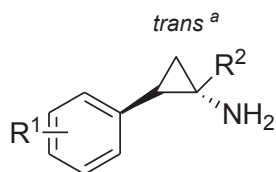
Scheme 3. Reagents and conditions: a) TEA, acetic anhydride, 90 °C, 6 h; b) 1. KOH, CH_3I , DMSO, 1 h; 2. $(\text{CH}_3)_3\text{SOI}$, NaH, DMSO, rt, 2 h; c) LiOH, THF/H₂O/MeOH (3:1:1), MW, 115 °C, 70 min; d) DPPA, TEA, *t*BuOH, 95 °C, 7 h; e) HCl (diethyl ether solution 2.0 M).

decrease of the activity. After the investigation at the *para* position, the bromine atom was introduced in the *meta* position of **1c**, but no noticeable improvement of the activity was observed (**44c**). Puzzled by the lack of a regular pattern for these preliminary substitutions, we also carried out modifications on scaffolds **1a** and **1e**, those endowed with the lower activity. With regard to **1e**, both *para*-bromo and *para*-chloro substitutions led to only a slight improvement in the activity (**46e** and **48e** vs **1e**), whereas the *para*-fluoro was found to be detrimental also in this context (**51e** vs **1e**). With regard to **1a**, the *para*-bromo substitution improved the activity over the parent compound by more than 6 times (**46a** vs **1a**), and the *para*-chloro substitution by more than 4 times (**48a** vs **1a**). Even more remarkable was the effect of the substitution at the *meta* position of the ring, where both bromine and chlorine yielded the most active compound of the series, with a more than 25-fold improvement of activity (**44a** and **45a** vs **1a**). However, also for this scaffold, fluorine at the *para* position failed to give a better inhibitory activity (**51a** vs **1a**).

Based on these data, the α -ethyl substituted series was chosen

as the template for further expansion of the SAR. The fluorine atom, detrimental at the *para* position, is still able to confer good activity when in the *meta* position (**47a**). Also a stronger EWG such as the trifluoromethyl, when at the *meta* position, was found to improve the activity of the parent compound (**49a** vs **1a**), although resulting about 4-times less active of **44a**. The trifluoromethyl group at the *para* position further decreased the activity of the molecule (**52a**), whereas the trifluoromethoxy substitution at the same position led to the least active derivative of the series (**57a**). To investigate how the electronic properties of the substituents could affect the activity, an EDG such as the methoxy group was introduced in the *meta* position. Although derivative **50a** was 6-fold more active than the parent compound (*cf* with **1a**), it was 4-fold less active than **44a** and the least active among the analogues of **1a** bearing a substitution at the *meta* position. Substitution at the *ortho* position with chlorine, bromine and fluorine led to compounds having a similar range of activities (**53a**, **54a**, and **55a**), about 10-fold less active than the lead **44a**. Finally, a disubstituted *para*-bromo, *meta*-fluoro derivative was prepared in order to see whether the merger

Table 1
Activity of the newly synthesized compounds against KDM1A.



Entry	R ¹	R ²	AVG IC ₅₀ ^b
1a ²⁴	H	Ethyl	0.779
1b ²⁴	H	Phenyl	0.161
1c ²⁴	H	PhEt	0.202
1d ²⁴	H	Naph	0.218
1e ²⁴	H	Benz	0.617
1f ²⁴	H	Methyl	1.72
44a	m-Br	Ethyl	0.031
45a	m-Cl	Ethyl	0.038
46a	p-Br	Ethyl	0.121
47a	m-F	Ethyl	0.079
48a	p-Cl	Ethyl	0.178
49a	m-CF ₃	Ethyl	0.118
50a	m-OCH ₃	Ethyl	0.123
51a	p-F	Ethyl	1.021
52a	p-CF ₃	Ethyl	0.248
53a	o-Cl	Ethyl	0.258
54a	o-Br	Ethyl	0.350
55a	o-F	Ethyl	0.352
56a	p-Br,m-F	Ethyl	0.035
57a	p-OCF ₃	Ethyl	1.159
46b	p-Br	Phenyl	0.047
48b	p-Cl	Phenyl	0.554
44c	m-Br	PhEt	0.094
46c	p-Br	PhEt	0.101
48c	p-Cl	PhEt	0.096
51c	p-F	PhEt	0.173
44d	m-Br	Naph	0.251
45d	m-Cl	Naph	0.158
46d	p-Br	Naph	0.279
51d	p-F	Naph	0.642
48d	p-Cl	Naph	0.263
46e	p-Br	Benz	0.187
48e	p-Cl	Benz	0.230
51e	p-F	Benz	1.053
63			na ^c
66			na

^a Compounds are a mixture of the 2 enantiomers.

^b Assays done in replicates (n ≥ 2). Mean values are shown and the standard deviations are <30% of the mean.

^c Compounds resulted inactive up to 100 μM.

of two favourable characteristics would have yielded a better derivative. Indeed, compound **56a** demonstrated to be one of the most potent derivative.

The spiro derivatives **63** and **66** were then planned and synthesized on the basis of some rational consideration: *a*) in general, rigidifying the ligand conformation might lead to a more favourable protein binding; *b*) they maintain the substituent at the α position, which is good for activity; and *c*) the substitution of the amino moiety with several substituents has been reported, in some cases, to be advantageous for the activity [40–42]. However, these two derivatives resulted inactive under our assay conditions. Several attempts to reduce the carbonyl moiety were made, using a number of reducing agents, but the corresponding spiro-piperidine and spiro-morpholine analogues could not be obtained.

The results of this investigation have given a number of new hints regarding the SAR for these α -substituted PCPA derivatives. In general, small functional groups attached at the β -phenyl ring of tranylcypromine analogues are well tolerated and lead to

molecules more active than the unadorned analogues. Bromo- and chloro-substitutions, either at the *para* or at the *meta* position, were found to confer the best activity in almost every scaffold used as the template, but this finding is more evident with α -ethyl PCPA. Given the mechanism of action of tranylcypromine derivatives, that involves the generation of a benzyl radical, it might be speculated that the stabilizing effect of these substituents play a role in the enhancement of the activity. An EDG such as the methoxy, although positively affecting the activity compared to the parent compound, is detrimental when compared to the most active compounds.

Interestingly, regardless of the substituent at the α -position of the PCPA derivative, with regard to the *para* position of the β -phenyl ring, the activity seems to be affected by the EWG properties of the substituents, and in particular weaker and larger electronegative substituents such as Br and Cl confer better activity than those smaller and with more pronounced electron-withdrawing properties, such as the F, CF₃, and OCF₃.

2.4. Computational analysis

What triggered our interest is the difference between the SAR established for compounds **1a–e**, where the ethyl at the α -position was found to confer the lowest activity to the PCPA derivatives, and that reported in this study, where α -ethyl-PCPA derivatives have the highest activity. To gain insights regarding these findings, a computational study was carried out. We addressed this observation from two different points of view: from one side, we tried to predict the binding mode of compounds **1a**, **1c**, **44a** and **44c** to see if the IC₅₀ values for the substituted ethyl derivatives are due to a different orientation in the binding site, compared with the unsubstituted α -ethyl and α -phenylethyl derivatives. On the other hand, we tried to assess if there are some differences in the reactivity profile of the molecules, calculating the HOMO–LUMO energy for the four compounds. We performed covalent docking of the derivatives to model the covalent adduct with FAD.

Adducts with C4a and N5 atoms were modelled, in agreement with previous studies on compounds belonging to the same series that suggested the initial formation of a cyclic adduct involving N5 and C4a that immediately rearranges into N5 or C4a adduct. In particular **1a** has been co-crystallized with KDM1A, thus we had an experimental evidence of the binding mode of this compound. Covalent docking results did not produce any clear indication to understand the reversal of the SAR previously established. We were able to reproduce with good accuracy the crystallographic adduct of compound **1a** (Fig. 2A, PDB 4UV9) but concerning the other derivatives, there was no unquestionable evidence that compound **44a** establishes stronger interactions or more favourable binding conformation. A different binding mode was observed for **44a** compared to **1a**, suggesting that presumably the presence of the bromine atom influences the binding mode (Fig. 2). Some valuable results came from the analysis of the HOMO–LUMO energy gap (ΔE). The HOMO–LUMO energy gap is associated with the reactivity of the molecules, with a smaller gap indicating a compound prompt to react. As it can be seen in Table 2 the calculated ΔE is higher for compound **1a** and it assumes the lowest value for compound **44a**. This is in good agreement with the average IC₅₀ value for these compounds, with compound **1a** showing a higher IC₅₀ value than **1c**, **44a** and **44c**. Therefore it can be speculated that the introduction of the bromine atom in *meta* position of the aromatic ring influences more the ethyl derivative than the phenylethyl one, which registered only a small variation of ΔE . The reduction of the HOMO–LUMO energy gap probably facilitates the direct opening of the cyclopropane ring, most likely through a radical mechanism, that was demonstrated to take place for these α -substituted PCPA derivatives instead of the enzymatic oxidation

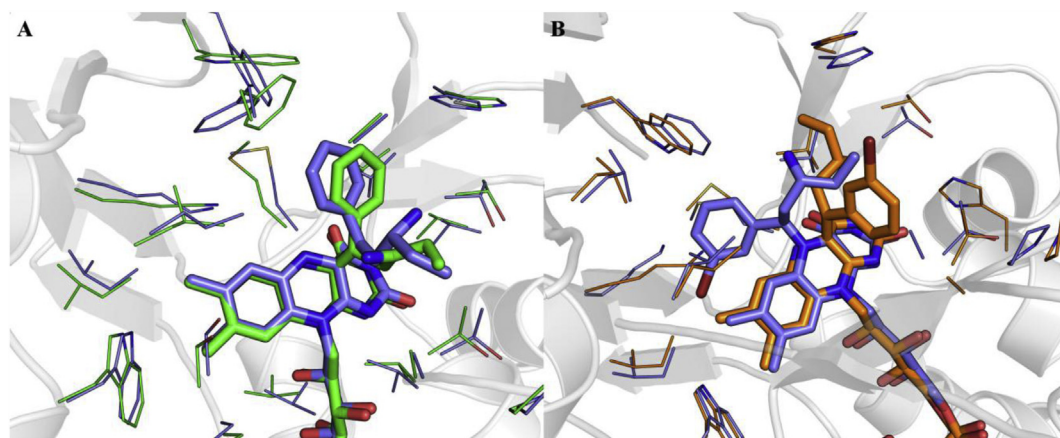


Fig. 2. A. Superposition of covalent binding pose of compound **1a** (in slate blue) to the crystallographic complex 4UV9 (in green). The amino group presents an opposite orientation in the covalent docking pose, but neither in the crystal structure nor in the docking experiment is interacting with a protein residue. B. Binding poses found for compound **44a** in covalent docking experiments; here are proposed the best binding pose of the C4a and N5 adducts (orange and slate respectively). (For interpretation of the references to colour in this figure legend, the reader is referred to the web version of this article.)

Table 2

HOMO LUMO energies, HOMO–LUMO gap calculated in vacuum and water for compounds **1a**, **1c**, **44a** and **44c**.

	Avg. IC ₅₀	Vacuum			Water		
		E _{HOMO} (eV)	E _{LUMO} (eV)	ΔE (eV)	E _{HOMO} (eV)	E _{LUMO} (eV)	ΔE (eV)
1a	0.779	−9.88	−4.64	5.24	−6.92	−0.61	6.31
1c	0.202	−9.34	−4.55	4.79	−6.86	−0.65	6.21
44a	0.031	−9.40	−4.72	4.68	−6.87	−0.89	5.98
44c	0.094	−9.34	−4.63	4.71	−6.87	−0.91	5.96

of the amino group.

3. Conclusion

In conclusion, the task of improving the inhibitory activity toward KDM1A of some α -substituted PCPA analogues was achieved with the synthesis of analogues bearing at the β -phenyl group several halogens and halogenated functional groups. In the majority of the cases, an improvement of the activity compared to the parent compound was noticed, with **44a**, the most active compound of the series, being 25-folds more active than **1a** and the most active of the α -substituted-PCPA derivatives. Probably, the electronegative character of these small functional groups plays a role in enhancing the activity. However, strong electronegative substituents are not tolerated at the *para* position. A computational investigation has led to the speculation that the reduction of the cyclopropane ring that occurs most likely through a radical mechanism. This fact may somehow explain the discrepancies between the SAR established in the previous paper and the data obtained in the present work.

Overall, this work highlights the fact that α -substituted tranylcypromine derivatives can undergo to various modification at the β -phenyl ring, with the aim to improve the inhibitory activity toward KDM1A. As such, further chemical manipulation of these substrates is ongoing in our laboratories.

4. Experimental protocol

4.1. Chemistry

All the reagents were purchased from Sigma–Aldrich, Alfa-

Aesar and Enamine at reagent purity and, unless otherwise noted, were used without any further purification. Dry solvents used in the reactions were obtained by distillation of technical grade materials over appropriate dehydrating agents. MCRs were performed using CEM Microwave Synthesizer-Discover model. Reactions were monitored by thin layer chromatography on silica gel-coated aluminium foils (silica gel on Al foils, SUPELCO Analytical, Sigma–Aldrich) at both 254 and 365 nm wavelengths. Where indicated, intermediates and final products were purified through Merck silica gel 60 flash chromatography (silica gel, 0.040–0.063 mm), using appropriate solvent mixtures.

¹H NMR and ¹³C NMR spectra were recorded on a BRUKER AVANCE spectrometer at 400 and 100 MHz respectively, or in a Varian 500 MHz with TMS as internal standard and a 300 K. ¹H NMR spectra are reported in this order: multiplicity and number of protons. Standard abbreviation indicating the multiplicity was used as follows: s = singlet, d = doublet, dd = doublet of doublets, t = triplet, q = quadruplet, m = multiplet and br = broad signal. HPLC/MS experiments were performed with HPLC: Agilent 1100 series, equipped with a Waters Symmetry C18, 3.5 μ m, 4.6 mm \times 75 mm column and MS: Applied Biosystem/MDS SCIEX, with API 150EX ion source, or, in alternative, HPLC–MS experiments were performed on an Acquity UPLC apparatus, equipped with a diode array and a Micromass SQD single quadrupole (Waters). HRMS experiments were performed with LTQ ORBITRAP XL THERMO.

All compounds were tested as 95% purity samples or higher (by HPLC/MS).

4.2. Molecular modelling

The covalent docking experiments have been performed using the apo crystal structure of KDM1A 2DW4 [43,44] and the covalent docking tool available in Prime 3.0 from Schrödinger [45]. Protein structure has been first prepared using the Protein Preparation tool [46]; ligands 3D structures with the correct stereochemistry and protonation state have been generated using LigPrep tool from Schrödinger [47]. A maximum number of ten poses have been generated for each ligand; after the covalent adducts were generated, a minimization of all the adducts including also protein residues within 6 Å has been carried out. The calculation of the HOMO–LUMO energy gap has been performed with Jaguar 8.2 included in Maestro9.6 Suite released by Schrodinger [48].

Geometry optimization of the compounds structures previously generated with LigPrep has been carried out using density functional theory (DFT) [49]. Initial geometries were minimized with the B3LYP hybrid density functional adopting the LACVP3P** basis set in vacuum and in water using the standard Poisson–Boltzmann solvation model [50].

4.3. General procedures

4.3.1. General procedure for the synthesis of phosphonates **a–e**

Ethyl 2-(diethoxyphosphoryl)acetate (1 eq) was added dropwise to a cooled suspension of NaH (1.1 eq) in dry DME (2 mL/mmol). After stirring at room temperature for 2 h the appropriate halide (1.1 eq) was added, and the mixture was stirred at 60 °C for additional 2 h. After quenching with ice–water, the mixture was extracted with ethyl acetate, and the combined organic layers were washed with H₂O and brine, dried over Na₂SO₄ and concentrated under reduced pressure. The crude material was purified through flash chromatography eluting dichloromethane–diethyl ether 95:5 to give the title compounds as colourless oils in yields ranging from 36% to 53%. Analytical data for compounds **a–e** matched the data published.

4.3.2. General procedure for the cyclopropanation (**2–15a, 4b, 2.4,6,9c, 2.3,4,9d, 4,6,9e**)

To a solution of the appropriate phosphorane (2 eq) in anhydrous DME (5 mL/mmol) at 25 °C, *n*-butyllithium (1.6 M in hexanes, 2 eq) was added dropwise over 5 min. After stirring for 30 min at the same temperature, the solution turned gradually to orange and the appropriate epoxide (1 eq) was added in one portion. The reaction was heated at 90 °C until consumption of the limiting reagent as determined by TLC, and then NH₄Cl is added to quench the reaction. The aqueous layer was extracted with ethyl acetate (3 × 15 mL), and the organic layers were washed with brine and dried (Na₂SO₄). After removal of the solvent *in vacuo*, the yellowish oil obtained was purified by flash column chromatography to give the title compounds as colourless oil. Yields, purification methods and analytical data are reported in details in the SI.

4.3.3. General procedure for the ester hydrolysis (**16–29a, 18b, 16,18,20,23c, 16,17,18,23d,18,20,23e, 69**)

The appropriate ester (1 eq) and LiOH·H₂O (4 eq) were dissolved in solution of THF/MeOH/H₂O (3/1/1, 1 mL/mmol) and heated in a microwave reactor at the following conditions: 100 °C; 250 psi; 300 W. The reaction mixture is then evaporated *in vacuo*, and the crude is washed with H₂O, acidified with HCl 2 N and extracted with ethyl acetate. After evaporation of the solvent, the product is used for the next reaction step without further purification. Using a similar procedure, but heating at 115 °C, compound **69** was obtained. Yields and LRMS are reported in the supporting information.

4.3.4. General procedure for the Curtius rearrangement (**30–43a, 32b, 30,32,34,37c, 30,31,32,37d, 32,34,37e, 70**)

to a solution of the appropriate acid (1 eq) in *tert*-butanol (10 mL/mmol), triethylamine (1.3 eq) and diphenylphosphorylazide (1.1 eq) were added, and the mixture was stirred at 90 °C overnight. After cooling, the reaction mixture was concentrated under reduced pressure and then partitioned between saturated Na₂CO₃ aqueous solution (30 mL) and ethyl acetate (3 × 10 mL). The combined organic layers were washed with brine, dried (Na₂SO₄) and concentrated under reduced pressure to give a yellowish material that is purified through flash chromatography on silica gel to give the title compounds. Yields, purification methods and other analytical data are reported in details in the SI.

4.3.5. General procedure for BOC hydrolysis (**44–57a, 46,48b, 44,46,48,51c, 44,45,46,51d, 46,48,51e**)

To a diethyl ether solution (0.5 mL/mmol) of the appropriate BOC-protected derivative (1 eq), maintained at 0 °C, either HCl 4 N (10 eq) or a saturated HCl solution in ethyl acetate (1 mL/mmol) were added. The reaction mixture was stirred at room temperature until consumption of the starting material (12–36 h), as determined by TLC, and then the solvent is evaporated under reduced pressure. The white solid formed is washed with diethyl ether, to give the title compounds as hydrochloride salts pure enough to be submitted for biological assay. Yields, ¹H NMR other analytical data are reported in details in the SI.

4.3.6. Diethyl 2-benzylidenemalonate (**58**)

A solution of diethyl malonate (5 g; 47 mmol), benzaldehyde (5.7 mL; 38 mmol), piperidine (230 μL; 2.35 mmol) and acetic acid (130 μL; 2.35 mmol) in anhydrous toluene (40 mL) were heated to reflux for 24 h. The solvent was evaporated under reduced pressure and the residue was taken up in ethyl acetate and washed with water (3 × 10 mL), brine and dried over Na₂SO₄. After evaporation of the solvent, the crude material was purified through a chromatography column eluting petroleum ether–ethyl acetate 85:15, to yield the desired product as a colourless oil. Yield: 79%. ¹H NMR (400 MHz-CDCl₃) □ = 1.14–1.22 (m, 6H), 3.26–3.28 (m, 1H), 4.06–4.26 (m, 4H), 7.28–7.77 (m, 5H).

4.3.7. Diethyl 2-phenylcyclopropane-1,1-dicarboxylate (**59**)

Under hydrogen atmosphere, trimethylsulfoxonium iodide (9 g; 40 mmol) was added in one portion to a stirred suspension of sodium hydride (1.63 g; 40 mmol) in anhydrous DMSO (90 mL), and the suspension was stirred till the frothing ceased. The resulting yellow mixture was cooled to 0 °C and a solution of diethyl 2-benzylidenemalonate **58** (9.44 g; 37 mmol) in anhydrous DMSO (10 mL) was added portionwise. The reaction mixture was stirred for 15 min at the same temperature and then allowed to react at room temperature until the TLC showed the complete consumption of the starting material. The mixture was then poured in ice water and extracted with ethyl acetate. The combined organic layers were washed with brine (3 × 10 mL), dried (Na₂SO₄) and concentrated under reduced pressure to give a yellowish oil that is purified by chromatography column eluting petroleum ether–ethyl acetate 9:1, yielding compound **59** as a colourless oil. Yield: 98%. ¹H NMR (300 MHz-CDCl₃) □ = 0.19 (t, J = 7.11 Hz, 3H), 1.24 (t, J = 7.14 Hz, 3H), 1.64 (q, J = 5.13 Hz, 1H), 2.13 (q, J = 5.16 Hz, 1H), 3.17 (t, J = 8.52 Hz, 1H), 3.78 (q, J = 7.14 Hz, 2H), 4.19 (q, J = 6 Hz, 2H), 7.17–7.27 (m, 5H).

Using a similar procedure, compound **68** (*trans* methyl 2-(4-chlorophenyl)-1-phenylcyclopropanecarboxylate) was obtained starting from the methyl ester of **67**. ¹H NMR (500 MHz-CDCl₃) □ = 7.64–6.59 (m, 9H), 3.85–3.24 (m, 3H), 3.15–2.75 (m, 1H), 2.42–2.09 (m, 1H), 1.93–1.57 (m, 1H).

4.3.8. 1-(Ethoxycarbonyl)-2-phenylcyclopropanecarboxylic acid (**60**)

A solution of NaOH (172 mg; 4.30 mmol) in EtOH (20 mL) was added to a solution of diethyl 2-phenylcyclopropane-1,1-dicarboxylate (1.026 g; 3.91 mmol) in ethanol at room temperature. The reaction mixture was stirred until consumption of the starting material according to TLC (3 days), after which the solvent was evaporated under reduced pressure, and the crude material washed with HCl 1 M (25 mL) and extracted with ethyl acetate (3 × 10 mL). The combined organic layers were washed with brine, dried (Na₂SO₄) and concentrated under reduced pressure to give a yellowish material that is used for the next reaction step without further purification.

Yield: 99%.

$^1\text{H NMR}$ (400 MHz- CDCl_3) \square = 0.56 (t, J = 5.6 Hz, 3H), 1.90 (s, 1H), 2.19 (d, J = 4.08 Hz, 1H), 3.19 (s, 1H), 3.61 (t, J = 6.6 Hz, 2H), 7.09–7.27 (m, 5H), 12.03 (s, 1H).

4.3.9. 1-((tert-Butoxycarbonyl)amino)-2-phenylcyclopropanecarboxylate (**61**)

Under nitrogen atmosphere, to a solution of **60** (3.064 g; 13 mmol) in anhydrous hexane (100 mL), diphenylphosphoryl azide (3.12 mL; 14 mmol), triethylamine (2 mL; 15 mmol) and tert-butanol (25 mL; 260 mmol) were added in this order and the mixture was allowed to react at reflux. After 18 h, a solution of Boc₂O (4.28 g; 19 mmol) in dry hexane (5 mL) was added, and the mixture was heated to reflux for additional 2 h. After cooling, the solvent was evaporated under reduced pressure, and the residue was taken up in ethyl acetate and washed with 5% citric acid (3 × 15 mL), water (3 × 10 mL), and saturated NaHCO₃ aqueous solution (3 × 10 mL). The combined organic layers were washed with brine, dried (Na₂SO₄) and concentrated under reduced pressure to give a yellowish material that is purified by chromatography column eluting petroleum ether–ethyl acetate 9:1, yielding the title compound as a white solid.

Yield: 77%.

$^1\text{H NMR}$ (400 MHz- CDCl_3) \square = 0.85 (s, 3H), 1.51 (s, 9H), 1.61–1.66 (m, 1H), 2.17 (m, 1H), 2.83 (t, J = 3.12 Hz, 1H), 3.81 (t, J = 3.8 Hz, 2H), 5.38 (s, 1H), 7.19–7.27 (m, 5H).

4.3.10. Ethyl 1-((2-((tert-butoxycarbonyl)amino)ethyl)amino)-2-phenylcyclopropanecarboxylate (**62**)

To a solution of ethyl **61** (1.5 g; 4.91 mmol) in dichloromethane (12 mL), trifluoroacetic acid (3 mL) was added dropwise at 0 °C. The solution, turned dark red, was stirred at room temperature for 1 h and then a solution of NaOH 1 M (10 mL) was added, and the organic layers separated, washed with brine, dried over Na₂SO₄ and evaporated under reduced pressure. The colourless product obtained after treatment was solubilized in dichloromethane (5 mL) and added dropwise to a solution of the N-Boc-2-aminoacetaldehyde (272 mg; 1.71 mmol) in dichloromethane (5 mL) at room temperature. After 15 min, sodium triacetoxyborohydride (906 mg; 4.26 mmol) was added in one portion and the reaction mixture was stirred at room temperature until the TLC showed the complete consumption of the amine. The solvent was evaporated under reduced pressure and the residue was taken up in ethyl acetate and washed with water (3 × 10 mL), brine and dried over Na₂SO₄. After evaporation of the solvent, the crude material was purified through a chromatography column eluting petroleum ether–ethyl acetate 6:4 to yield the title compound as a pale yellow oil.

Yield: 42%.

$^1\text{H NMR}$ (400 MHz- CDCl_3) \square = 0.75 (t, J = 7.08 Hz, 3H), 1.43–1.45 (m, 11H), 1.95 (q, J = 5.36 Hz, 1H), 2.64 (t, J = 8.52 Hz, 1H), 2.81–2.92 (m, 2H), 3.16–3.25 (m, 2H), 3.69–3.78 (m, 2H), 5.08 (s, 1H), 7.18–7.28 (m, 5H).

4.3.11. 1-Phenyl-4,7-diazaspiro[2.5]octan-8-one (**63**)

To a solution of compound **62** (240 mg; 0.68 mmol) in dichloromethane (2.5 mL), trifluoroacetic acid (0.5 mL) was added dropwise at 0 °C and the mixture was allowed to stir at room temperature for 1 h. A solution of KOH 10% (10 mL) was added dropwise to the reaction flask in an ice bath, and the stirring is continued for additional 2 h. The precipitated obtained is collected, and purified through flash chromatography column eluting dichloromethane–methanol 95:5 to yield the title compound as light pink solid.

Yield: 54%.

$^1\text{H NMR}$ (300 MHz- CDCl_3) \square = 1.38–1.43 (m, 1H), 1.73 (s, 1H), 2.13–2.17 (m, 1H), 2.45 (t, J = 8.38 Hz, 1H), 3.19–3.51 (m, 4H), 5.87 (s, 1H), 7.17–7.28 (m, 5H).

4.3.12. Tert-butyl (1-(hydroxymethyl)-2-phenylcyclopropyl) carbamate (**64**)

A suspension of lithium aluminium hydride (745 mg; 20 mmol) in dry THF (30 mL) was cooled to 0 °C and ethyl 1-((tert-butoxycarbonyl)amino)-2-phenylcyclopropanecarboxylate **61** (1.5 g; 4.9 mmol) solubilized in dry THF (10 mL) was added under nitrogen atmosphere. The reaction mixture was stirred at room temperature until TLC showed the consumption of the limiting reagent, and then a solution of NaOH 1 N (5 mL) was added and the organic phase extracted with ethyl acetate (3 × 30 mL). The combined organic layers were washed with brine, dried (Na₂SO₄) and concentrated under reduced pressure to give a yellowish oil that is purified by chromatography column eluting petroleum ether–ethyl acetate 9:1, yielding the title compound as a yellowish oil.

Yield: 89%.

$^1\text{H NMR}$ (300 MHz- CDCl_3) \square = 1.49 (s, 9H), 1.95 (q, J = 5.36 Hz, 1H), 2.50 (t, J = 7.35 Hz, 1H), 3.32 (d, J = 11.82 Hz, 1H), 3.45 (d, J = 11.91 Hz, 1H), 3.66–3.84 (m, 2H), 5.38 (s, 1H), 7.22–7.35 (m, 5H).

4.3.13. 2-Bromo-N-(1-(hydroxymethyl)-2-phenylcyclopropyl) acetamide (**65**)

Trifluoroacetic acid (2 mL) was added dropwise at 0 °C to a solution of ethyl 1-((tert-butoxycarbonyl)amino)-2-phenylcyclopropanecarboxylate **64** (1.027 g; 3.9 mmol) in dichloromethane (8 mL). After stirring at room temperature for 1 h, a solution of NaOH 1 N (3 mL) was added to the reaction mixture, and the organic layers were separated, washed with brine, dried over Na₂SO₄ and evaporated under reduced pressure. To a solution of the residue and triethylamine (940 μL ; 6.07 mmol) in anhydrous dichloromethane (25 mL) at 0 °C, a solution of bromoacetylchloride (509 μL ; 6.12 mmol) in dichloromethane (10 mL) was added dropwise. The reaction mixture was stirred until consumption of the limiting reagent, as determined by TLC. The reaction mixture was then treated with HCl 1 N (3 mL), and the organic layers separated, washed with brine, dried over Na₂SO₄ and evaporated under reduced pressure, to give a crude material that is purified through flash chromatography eluting dichloromethane–methanol 97:3, yielding **65** as a pale yellow oil. Yield: 34%. $^1\text{H NMR}$ (400 MHz- CDCl_3) \square = 1.35–1.49 (m, 2H), 1.99 (s, 2H), 2.75 (q, J = 7.52 Hz, 1H), 3.41–3.52 (m, 1H), 4.11 (s, 2H), 7.18 (s, 1H), 7.25–7.34 (m, 5H).

4.3.14. 1-Phenyl-7-oxa-4-azaspiro[2.5]octan-5-one (**66**)

under nitrogen atmosphere, to a suspension of NaH (904 mg; 1.15 mmol) in dry THF (25 mL) at 0 °C, 2-bromo-N-(1-(hydroxymethyl)-2-phenylcyclopropyl)acetamide **65** (311 mg; 1.15 mmol), solubilized in dry THF (5 mL), was added dropwise. The mixture was stirred at the same temperature for 2 h and then poured into ice water, and extracted with ethyl acetate (3 × 10 mL). The combined organic layers were washed with brine, dried (Na₂SO₄) and concentrated under reduced pressure to give a yellowish oil that is purified by chromatography column eluting petroleum ether–ethyl acetate 8:2, yielding compound **66** as a pale yellow oil. Yield: 98%. $^1\text{H NMR}$ (300 MHz- CDCl_3) \square = 1.38–1.43 (m, 1H), 2.13–2.17 (m, 1H), 2.45 (t, J = 8.38 Hz, 1H), 3.19–3.51 (m, 4H), 5.87 (s, 1H), 7.17–7.28 (m, 5H).

4.3.15. (E)-3-(4-Chlorophenyl)-2-phenyl-prop-2-enoic acid (**67**)

A solution of 4-Cl-benzaldehyde (2.0 g, 14.23 mmol), phenylacetic acid (1.9 g, 14.23 mmol) and triethylamine (2.0 mL, 14.23 mmol) in acetic anhydride (10 mL) was stirred at 90 °C. After 6 h of heating the reaction was cooled to 25 °C. Diethyl ether

(30 mL) and water (20 mL) were added: precipitation of a white solid occurred. The resulting organic phase was extracted with 10% w/v of aqueous NaOH (3 × 10 mL). The combined aqueous layers were acidified to pH 2 using concentrated hydrochloric acid; the precipitate was filtered off and washed with water and dried obtaining (E)-3-(4-chlorophenyl)-2-phenyl-prop-2-enoic acid (2.3 g, 63% yield) as a white solid. ¹H NMR (500 MHz, DMSO-d₆) δ = 12.78 (s, 1H), 7.74 (s, 1H), 7.41–7.32 (m, 3H), 7.29–7.24 (m, J = 8.3 Hz, 2H), 7.18–7.14 (m, 2H), 7.07–7.02 (m, J = 8.8 Hz, 2H).

4.3.16. (E)-Methyl 2,3-diphenylacrylate

(E)-3-(4-chlorophenyl)-2-phenyl-prop-2-enoic acid (2.3 g, 8.891 mmol) and powdered KOH (0.7 g, 12.00 mmol) were dissolved in dimethylsulfoxide (3 mL) and the mixture was stirred for 1 h at room temperature. Iodomethane (1.9 g, 13.00 mmol) was then added and the solution was stirred for 1 h. The reaction, was diluted with water and, precipitation occurred. The suspension was filtered off and the resulting solid was washed with water and dried obtaining methyl (E)-3-(4-chlorophenyl)-2-phenyl-prop-2-enoate (2.2 g, 93% yield) as a white solid. ¹H NMR (500 MHz, CDCl₃) δ = 7.80 (s, 1H), 7.43–7.35 (m, 3H), 7.23–7.18 (m, J = 2.2, 7.1 Hz, 2H), 7.15–7.11 (m, J = 8.3 Hz, 2H), 6.99–6.93 (m, J = 8.8 Hz, 2H), 3.81 (s, 3H). MS (ESI): *m/z*: 273 [M+H].

4.4. Biological assays

4.4.1. KDM1A (LSD1) enzyme inhibition assay

The complex of human recombinant KDM1A/CoREST protein was produced in *Escherichia coli* as separate proteins and co-purified following previously reported procedures [17]. The experiments were performed in 96 well half area white plates (cat. 3693, Corning, Corning, NY) using a mono-methylated H3–K4 peptide containing 21 amino acids (custom synthesis done by Thermo Scientific) as substrate and in a 40 μL volume of 50 mM TRIS–HCl, pH 8.0 and 0.05 mg/ml BSA buffer. The peptide purity was >95% as checked by analytical high-pressure liquid chromatography and mass spectrometry. The demethylase activity was estimated under aerobic conditions and at RT by measuring the release of H₂O₂ produced during the catalytic process by the Amplex[®] UltraRed detection system coupled with horseradish peroxidase (HRP). Briefly, 20 nM of KDM1A/CoREST complex was incubated at RT for 15 min in the absence and/or the presence of various concentrations of the inhibitors, 50 μM Amplex[®] UltraRed (Life Technologies) and 0.023 μM HRP (Sigma) in 50 mM Tris–HCl pH8.0 and 0.05 mg/ml BSA. The inhibitors were tested twice in duplicates at each concentration. Tranylcpromine (Sigma) was used as control. After preincubation of the enzyme with the inhibitor, the reaction was initiated by addition of 4.5 μM of mono-methylated H3–K4 peptide. The conversion of the Amplex[®] Ultra Red reagent to Amplex[®] UltroxRed was monitored by fluorescence (excitation at 510 nm, emission at 595 nm) for 12 min and by using a microplate reader (Infinite 200, Tecan Group, Switzerland). Arbitrary units were used to measure the level of H₂O₂ produced in the absence and/or in the presence of inhibition. The maximum demethylase activity of KDM1A/CoREST was obtained in the absence of inhibitors and corrected for background fluorescence in the absence of KDM1A/CoREST. The IC₅₀ was calculated using GraphPad Prism version 4.0 (GraphPad Software, San Diego, CA).

Author contributions

The manuscript was written through contributions of all authors. All authors have given approval to the final version of the manuscript.

Acknowledgements

Giuseppe Baratto is acknowledged for the help in the synthesis of derivatives. This work was supported by Fondazione Cariplo (2010.0778), AIRC (IG-11342), MIUR (Progetto Epigen and RF-2010-2318330), FIRBRBFR10ZJQT, Sapienza Ateneo Project 2012, IIT-Sapienza Project, FP7 Project BLUEPRINT/282510, and Regione Lombardia, Fondo per la Promozione di Accordi Istituzionale, Bando di Invito di cui al Decreto n. 4779 del 14/05/2009, Progetto DiVA.

Appendix A. Supplementary data

Supplementary data related to this article can be found at <http://dx.doi.org/10.1016/j.ejmech.2014.12.032>.

References

- [1] S.L. Berger, *Histone modifications in transcriptional regulation*, *Curr. Opin. Genet. Dev.* 12 (2002) 142–148.
- [2] T. Jenuwein, C.D. Allis, Translating the histone code, *Science* 293 (2001) 1074–1080, <http://dx.doi.org/10.1126/science.1063127>.
- [3] M.R. Hübner, M.A. Eckersley-Maslin, D.L. Spector, Chromatin organization and transcriptional regulation, *Curr. Opin. Genet. Dev.* 23 (2013) 89–95, <http://dx.doi.org/10.1016/j.gde.2012.11.006>.
- [4] K. Mekhail, D. Moazed, The nuclear envelope in genome organization, expression and stability, *Nat. Rev. Mol. Cell. Biol.* 11 (2010) 317–328, <http://dx.doi.org/10.1038/nrm2894>.
- [5] A.P. Feinberg, B. Vogelstein, Hypomethylation distinguishes genes of some human cancers from their normal counterparts, *Nature* 301 (1983) 89–92, <http://dx.doi.org/10.1038/301089a0>.
- [6] V.M. Richon, Cancer biology: mechanism of antitumor action of vorinostat (suberoylanilide hydroxamic acid), a novel histone deacetylase inhibitor, *Br. J. Cancer* 95 (2006) S2–S6, <http://dx.doi.org/10.1038/sj.bjc.6603463>.
- [7] H. Nakajima, Y.B. Kim, H. Terano, M. Yoshida, S. Horinouchi, FR901228, a potent antitumor antibiotic, is a novel histone deacetylase inhibitor, *Exp. Cell Res.* 241 (1998) 126–133, <http://dx.doi.org/10.1006/excr.1998.4027>.
- [8] M. Haberland, R.L. Montgomery, E.N. Olson, The many roles of histone deacetylases in development and physiology: implications for disease and therapy, *Nat. Rev. Genet.* 10 (2009) 32–42, <http://dx.doi.org/10.1038/nrg2485>.
- [9] A.J.M. de Ruijter, A.H. van Gennip, H.N. Caron, S. Kemp, A.B.P. van Kuilenburg, Histone deacetylases (HDACs): characterization of the classical HDAC family, *Biochem. J.* 370 (2003) 737–749, <http://dx.doi.org/10.1042/BJ20021321>.
- [10] P. Filippakopoulos, S. Knapp, Targeting bromodomains: epigenetic readers of lysine acetylation, *Nat. Rev. Drug Discov.* 13 (2014) 337–356, <http://dx.doi.org/10.1038/nrd4286>.
- [11] R.M. Labbe, A. Holowatyj, Z.-Q. Yang, Histone lysine demethylase (KDM) subfamily 4: structures, functions and therapeutic potential, *Am. J. Transl. Res.* 6 (2013) 1–15.
- [12] C. Martin, Y. Zhang, The diverse functions of histone lysine methylation, *Nat. Rev. Mol. Cell. Biol.* 6 (2005) 838–849, <http://dx.doi.org/10.1038/nrm1761>.
- [13] D. Rotili, A. Mai, Targeting histone demethylases a new avenue for the fight against cancer, *Genes. Cancer* 2 (2011) 663–679, <http://dx.doi.org/10.1177/1947601911417976>.
- [14] N. Mosammamaparast, Y. Shi, Reversal of histone methylation: biochemical and molecular mechanisms of histone demethylases, *Annu. Rev. Biochem.* 79 (2010) 155–179, <http://dx.doi.org/10.1146/annurev.biochem.78.070907.103946>.
- [15] A. Karytinov, F. Forneris, A. Profumo, G. Ciossani, E. Battaglioli, C. Binda, et al., A novel Mammalian flavin-dependent histone demethylase, *J. Biol. Chem.* 284 (2009) 17775–17782, <http://dx.doi.org/10.1074/jbc.M109.003087>.
- [16] C. Loenarz, C.J. Schofield, Expanding chemical biology of 2-oxoglutarate oxygenases, *Nat. Chem. Biol.* 4 (2008) 152–156, <http://dx.doi.org/10.1038/nchembio0308-152>.
- [17] F. Forneris, C. Binda, E. Battaglioli, A. Mattevi, LSD1: oxidative chemistry for multifaceted functions in chromatin regulation, *Trends Biochem. Sci.* 33 (2008) 181–189, <http://dx.doi.org/10.1016/j.tibs.2008.01.003>.
- [18] Y. Shi, F. Lan, C. Matson, P. Mulligan, J.R. Whetstone, P.A. Cole, et al., Histone demethylation mediated by the nuclear amine oxidase homolog LSD1, *Cell* 119 (2004) 941–953, <http://dx.doi.org/10.1016/j.cell.2004.12.012>.
- [19] D.N. Ciccone, H. Su, S. Hevi, F. Gay, H. Lei, J. Bajko, et al., KDM1B is a histone H3K4 demethylase required to establish maternal genomic imprints, *Nature* 461 (2009) 415–418, <http://dx.doi.org/10.1038/nature08315>.
- [20] T. Schenk, W.C. Chen, S. Göllner, L. Howell, L. Jin, K. Hebestreit, et al., Inhibition of the LSD1 (KDM1A) demethylase reactivates the all-trans-retinoic acid differentiation pathway in acute myeloid leukemia, *Nat. Med.* 18 (2012) 605–611, <http://dx.doi.org/10.1038/nm.2661>.
- [21] J.H. Schulte, S. Lim, A. Schramm, N. Friedrichs, J. Koster, R. Versteeg, et al., Lysine-specific demethylase 1 is strongly expressed in poorly differentiated neuroblastoma: implications for therapy, *Cancer Res.* 69 (2009) 2065–2071, <http://dx.doi.org/10.1158/0008-5472.CAN-08-1735>.

- [22] F. Crea, L. Sun, A. Mai, Y.T. Chiang, W.L. Farrar, R. Danesi, et al., The emerging role of histone lysine demethylases in prostate cancer, *Mol. Cancer* 11 (2012) 52, <http://dx.doi.org/10.1186/1476-4598-11-52>.
- [23] T. Suzuki, N. Miyata, Lysine demethylases inhibitors, *J. Med. Chem.* 54 (2011) 8236–8250, <http://dx.doi.org/10.1021/jm201048w>.
- [24] P. Vianello, O.A. Botrugno, A. Cappa, G. Ciossani, P. Dessanti, A. Mai, et al., Synthesis, biological activity and mechanistic insights of 1-substituted cyclopropylamine derivatives: a novel class of irreversible inhibitors of histone demethylase KDM1A, *Eur. J. Med. Chem.* 86 (2014) 352–363, <http://dx.doi.org/10.1016/j.ejmech.2014.08.068>.
- [25] D.M.Z. Schmidt, D.G. McCafferty, trans-2-Phenylcyclopropylamine is a mechanism-based inactivator of the histone demethylase LSD1, *Biochem. Mosc.* 46 (2007) 4408–4416, <http://dx.doi.org/10.1021/bi0618621>.
- [26] M.G. Lee, C. Wynder, D.M. Schmidt, D.G. McCafferty, R. Shiekhhattar, Histone H3 lysine 4 demethylation is a target of nonselective antidepressive medications, *Chem. Biol.* 13 (2006) 563–567, <http://dx.doi.org/10.1016/j.chembiol.2006.05.004>.
- [27] M. Yang, J.C. Culhane, L.M. Szewczuk, P. Jalili, H.L. Ball, M. Machius, et al., Structural basis for the inhibition of the LSD1 histone demethylase by the antidepressant trans-2-phenylcyclopropylamine, *Biochem. Mosc.* 46 (2007) 8058–8065, <http://dx.doi.org/10.1021/bi700664y>.
- [28] J.C. Culhane, D. Wang, P.M. Yen, P.A. Cole, Comparative analysis of small molecules and histone substrate analogues as LSD1 lysine demethylase inhibitors, *J. Am. Chem. Soc.* 132 (2010) 3164–3176, <http://dx.doi.org/10.1021/ja909996p>.
- [29] E. Metzger, M. Wissmann, N. Yin, J.M. Müller, R. Schneider, A.H.F.M. Peters, et al., LSD1 demethylates repressive histone marks to promote androgen-receptor-dependent transcription, *Nature* 437 (2005) 436–439, <http://dx.doi.org/10.1038/nature04020>.
- [30] Y. Huang, E. Greene, T.M. Stewart, A.C. Goodwin, S.B. Baylin, P.M. Woster, et al., Inhibition of lysine-specific demethylase 1 by polyamine analogues results in reexpression of aberrantly silenced genes, *Proc. Natl. Acad. Sci.* 104 (2007) 8023–8028, <http://dx.doi.org/10.1073/pnas.0700720104>.
- [31] S.K. Sharma, Y. Wu, N. Steinbergs, M.L. Crowley, A.S. Hanson, R.A. Casero, et al., (Bis)urea and (Bis)thiourea inhibitors of lysine-specific demethylase 1 as epigenetic modulators, *J. Med. Chem.* 53 (2010) 5197–5212, <http://dx.doi.org/10.1021/jm100217a>.
- [32] J. Wang, F. Lu, Q. Ren, H. Sun, Z. Xu, R. Lan, et al., Novel histone demethylase LSD1 inhibitors selectively target cancer cells with pluripotent stem cell properties, *Cancer Res.* 71 (2011) 7238–7249, <http://dx.doi.org/10.1158/0008-5472.CAN-11-0896>.
- [33] V. Sorna, E.R. Theisen, B. Stephens, S.L. Warner, D.J. Bearss, H. Vankayalapati, et al., High-throughput virtual screening identifies novel N'-(1-phenylethylidene)-benzohydrazides as potent, specific, and reversible LSD1 inhibitors, *J. Med. Chem.* 56 (2013) 9496–9508, <http://dx.doi.org/10.1021/jm400870h>.
- [34] N. Johnson, J. Kasparec, W. Miller, M. Rouse, D. Suarez, X. Tian, 2012, Cyclopropylamines as Lsd1 Inhibitors, WO/2012/135113, http://patentscope.wipo.int/search/en/detail.jsf?docId=WO2012135113&recNum=66&docAn=US2012030552&queryString=EN_ALL:nmr%20AND%20PA:glaxosmithkline&maxRec=557 (accessed 26.09.14).
- [35] A. Ortega Muñoz, M.C.T. Fyfe, M. Martinell Pedemonte, M. de los Á. Estiarte Martínez, N. Valls Vidal, G. Kurz, et al., 2012, (Hetero)aryl Cyclopropylamine Compounds as Lsd1 Inhibitors, WO/2013/057320, <http://patentscope.wipo.int/search/en/detail.jsf?docId=WO2013057320&recNum=2&docAn=EP2012070898&queryString=&maxRec=17259> (accessed 26.09.14).
- [36] A. Ortega Muñoz, M.C.T. Fyfe, M. Martinell Pedemonte, M. de los Á. Estiarte Martínez, N. Valls Vidal, G. Kurz, et al., 2013, (Hetero)aryl Cyclopropylamine Compounds as Lsd1 Inhibitors, WO/2013/057322, <http://patentscope.wipo.int/search/en/WO2013057322> (accessed 26.09.14).
- [37] D.M.Z. Schmidt, D.G. McCafferty, trans-2-Phenylcyclopropylamine is a mechanism-based inactivator of the histone demethylase LSD1, *Biochem. Mosc.* 46 (2007) 4408–4416, <http://dx.doi.org/10.1021/bi0618621>.
- [38] C.D. Bray, F. Minicone, Stereocontrolled synthesis of quaternary cyclopropyl esters, *Chem. Commun.* 46 (2010) 5867–5869, <http://dx.doi.org/10.1039/C0CC01333A>.
- [39] M. Shiozaki, K. Maeda, T. Miura, Y. Ogoshi, J. Haas, A.M. Fryer, et al., Novel N-substituted 2-phenyl-1-sulfonylamino-cyclopropane carboxylates as selective ADAMTS-5 (aggrecanase-2) inhibitors, *Bioorg. Med. Chem. Lett.* 19 (2009) 1575–1580, <http://dx.doi.org/10.1016/j.bmcl.2009.02.024>.
- [40] N. Guibourt, M.A. Ortega, L.J. Castro-Palomino, 2010, Patent Appl. WO 2010043721.
- [41] N. Guibourt, M.A. Ortega, L.J. Castro-Palomino, 2010, Patent Appl. WO 2010084160.
- [42] M.A. Ortega, L.J. Castro-Palomino, M.C.T. Fyfe, 2011, Patent Appl. WO 2011035941.
- [43] S. Mimasu, T. Sengoku, S. Fukuzawa, T. Umehara, S. Yokoyama, Crystal structure of histone demethylase LSD1 and tranlycypromine at 2.25 Å, *Biochem. Biophys. Res. Commun.* 366 (2008) 15–22, <http://dx.doi.org/10.1016/j.bbrc.2007.11.066>.
- [44] F.C. Bernstein, T.F. Koetzle, G.J. Williams, E.F. Meyer, M.D. Brice, J.R. Rodgers, et al., The Protein Data Bank: a computer-based archival file for macromolecular structures, *J. Mol. Biol.* 112 (1977) 535–542.
- [45] Prime, version 3.0, Schrödinger, LLC, New York, NY, 2011.
- [46] Protein Preparation Wizard, Schrödinger, LLC, New York, NY, 2011.
- [47] LigPrep, version 2.8, Schrödinger, LLC, New York, NY, 2013.
- [48] Jaguar, version 8.2, Schrödinger, LLC, New York, NY, 2013.
- [49] P. Geerlings, F. De Proft, W. Langenaeker, Conceptual density functional theory, *Chem. Rev.* 103 (2003) 1793–1874, <http://dx.doi.org/10.1021/cr990029p>.
- [50] B. Marten, K. Kim, C. Cortis, R.A. Friesner, R.B. Murphy, M.N. Ringnalda, et al., New model for calculation of solvation free energies: correction of self-consistent reaction field continuum dielectric theory for short-range hydrogen-bonding effects, *J. Phys. Chem.* 100 (1996) 11775–11788, <http://dx.doi.org/10.1021/jp953087x>.